33RD INTERNATIONAL COSMIC RAY CONFERENCE, RIO DE JANEIRO 2013
THE ASTROPARTICLE PHYSICS CONFERENCE

ICRC 2013

Search for high-energy emission from GRBs with the HAWC Observatory

K. SPARKS[1], FOR THE HAWC COLLABORATION.

[1] *Department of Physics, Pennsylvania State University, University Park, PA, USA*

kjs361@psu.edu

Abstract: A second generation water Cherenkov detector, the High Altitude Water Cherenkov (HAWC) Observatory is currently being constructed in Sierra Negra, Mexico at an altitude of 4100 m asl. With higher altitude than its predecessor Milagro, HAWC will be almost two orders of magnitude more sensitive to GRBs at 100 GeV. Due to its wide instantaneous field of view (~ 2 sr) and long duty cycle, this Extensive Air Shower detector can observe the beginning of the prompt phase of GRBs without needing to slew. HAWC is sensitive to showers in the sub-TeV to TeV energy range and will be able to help constrain the shape and cutoff of high-energy GRB spectra, especially in conjunction with observations from other detectors such as Fermi. Data taking with a partially built array began in 2012. With only 10% of the array completed, HAWC already provides a substantial improvement over Milagro's sensitivity to GRBs. We present the results of a search for high energy emission from GRBs detected by other instruments using HAWC data.

Keywords: HAWC, gamma-ray bursts, very high-energy gamma rays.

1 Introduction

Gamma-ray bursts (GRBs) are extremely powerful transient events that occur at cosmic distances. The exact origins are still unknown, but GRBs are thought to occur during neutron star-neutron star or neutron star-black hole mergers [1, 2] or the core collapse of massive stars [3, 4]. A jetted, highly relativistic fireball interacting with itself or the surrounding interstellar matter, forming internal and external shocks in which Fermi-acceleration takes place, delivers a plausible explanation of the non-thermal spectrum of GRBs [5, 6, 7]. The emission mechanism for the high-energy gamma rays is not yet completely understood.

Observations of energy spectra of GRBs can provide information about the intervening space between the burst and Earth as well as about the source itself. As gamma rays propagate through the interstellar media, they interact with the extra-galactic background light (EBL), which can cause attenuation via pair-production [8]. The density of the EBL can consequently be probed with the observation of a high-energy cutoff. GRB prompt emission is typically described by the Band function [9], two power laws joined by an exponential cutoff. However, recent observations have shown that a Band function alone cannot sufficiently describe many high-energy gamma-ray bursts [10, 11].

The release of the *Fermi* LAT Gamma-Ray Burst Catalog [12] earlier this year summarized knowledge of the high-energy component of LAT GRBs. The *Fermi* Gamma Ray Space Telescope consists of two detectors, the Large Area Telescope (LAT), operating at energies between $\sim$20 MeV and more than 300 GeV, and the Gamma-ray Burst Monitor (GBM), whose energy range is lower at 8 keV to 40 MeV. Thirty-five GRBs were detected by LAT in a three-year period starting in August 2008.

From these detections, we garner more information about the characteristics of high-energy GRBs. LAT-detected emission is commonly delayed with respect to the lower energy counterpart detected by GBM. Additionally, a temporally extended phase during which LAT flux decays following a single or broken power law with index close to $F_\nu \propto t^{-1}$ is observed. This extended emission is consistent with that expected from forward shock emission from a relativistic blast wave and favors an adiabatic fireball model over a radiative one. Finally, joint GBM-LAT spectral fits to all LAT GRBs require a power-law component in addition to the Band function to fit the bursts.

As a space-based instrument, *Fermi* LAT's effective area is limited by the size of the satellite. Due to the paucity of the flux, observation of the highest energy gamma rays requires a larger effective area. To do this, two different classes of ground-based detectors exist: Imaging Atmospheric Cherenkov Telescopes (IACTs) [13] and Extensive Air Shower (EAS) particle detector arrays [14]. IACTs have very good angular and energy resolution enabling a high degree of sensitivity. However, they can only observe on clear, moonless nights ($\sim$10% duty cycle) and have a small field of view ($< 5^\circ$). The prompt phase of a GRB is often missed by IACTs due to slewing. EAS detectors, such as the High Altitude Water Cherenkov (HAWC) Observatory, have a nearly 100% duty cycle and a large field of view (~ 2 sr), thus allowing for easier detection of the prompt phase of a GRB.

2 The HAWC observatory

Located at 4100 m in Sierra Negra, Mexico, HAWC will consist of 300 7.3 m wide and 4.5 m deep water tanks when completed. There are three 20 cm photomultiplier tubes (PMTs) and one 25 cm high quantum efficiency PMT at the bottom of each tank. Charged particles from an extensive air shower are detected when they pass through each tank and emit Cherenkov radiation. HAWC data is collected by two data acquisition systems (DAQs). The main DAQ measures the arrival time and time over threshold (TOT) of PMT pulses, hence providing information for the reconstruction of the shower core, direction and lateral distribution, which in turn helps to determine the species of primary particle and its energy. A secondary DAQ, the scaler system, operates in a PMT pulse counting mode [15]

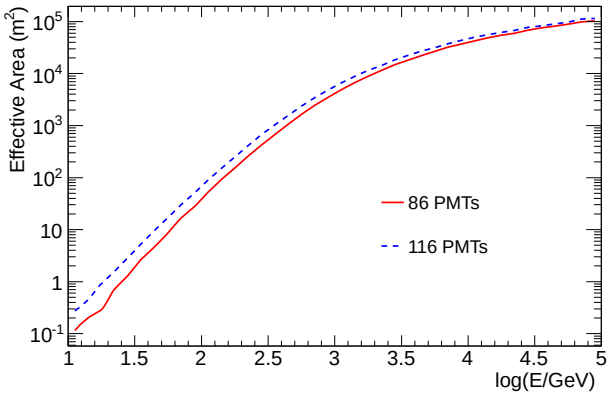

Fig. 1: Effective area of HAWC main DAQ as a function of γ-ray energy for showers $< 45^\circ$ zenith. A trigger threshold of nHit $\geq$10, corresponding to a rate of $\sim$7 kHz, is assumed. Showers reconstructed with $> 4^\circ$ error are excluded. No gamma-hadron separation cut is applied.

and is sensitive to gamma ray and cosmic ray (i.e. due to solar activity) transient events that produce a sudden increase or decrease in counting rates with respect to those produced by atmospheric showers and noise. GRB results discussed in the following sections are primarily from the main DAQ while results from the scaler DAQ are presented in [16]. For more information on the HAWC observatory see [17] and [18] in these proceedings.

3 VAMOS / HAWC GRB selection

HAWC's Verification and Assessment Measuring of Observatory Subsystem (VAMOS) prototype took data from September 2011 to June 2012 with $\sim$30% live time. VAMOS consisted of 6 tanks with 31 PMTs.

Based on GCN circulars[1], two intense GRBs that occurred within VAMOS' field-of-view (FoV) (zenith angle $< 45^\circ$) and uptime were selected for analysis: GRB 111016B and GRB 120328B. Both bursts were discovered by IPN (GCN circulars 12452 and 13157), with a gamma ray fluence reported by Konus-Wind in excess of 10^{-4} erg/cm^2 in both cases. In addition to the low-energy gamma rays seen by GBM, *Fermi* LAT reported a detection of high-energy emission from GRB 120328B (GCN circular 13165). For VAMOS, GRB 111016B had a zenith angle of 32°, while GRB 120328B was at a less favorable 41°. No redshift information is available for these GRBs.

Regular data taking with the partially constructed HAWC array began in September 2012. Approximately 145 days of live time was accumulated during the first 7 months (September through April) by the growing experiment. The dataset used in this analysis contains events with a maximum of 86 to 114 PMTs, triggered at a rate of approximately 7 kHz. The effective area for the complete HAWC array was shown in [17] while Figure 1 shows the relevant effective area for the following analysis.

Based on the *Fermi* GBM[2] and Swift[3] GRB catalogs, we selected 12 bursts that were in the FoV of HAWC (zenith angle $< 45^\circ$) during its main DAQ uptime and had a localization accuracy better than 5° (for GBM bursts). This includes GRB 130504C (GCN circulars 14574, 14583, and 14587), a extremely bright burst with long lasting emission from which LAT detected a photon of $\sim$5 GeV. The results of this selection process are summarized in Table 1.

The nearby super-luminous burst GRB 130427A [19] was at 57° zenith in HAWC's FoV and setting at the time of its GBM trigger. The main DAQ was not taking data at the time, but the scaler DAQ was running. A full analysis of this burst can be found in [16].

4 GRB search results

We first analyzed the main DAQ VAMOS data for GRB 111016B to establish if an intense high-energy emission was present. The number of air showers detected during a 155 s time interval around the GRB (including 5 s before T0 = 22:41:40 UT plus the reported GRB duration) and reconstructed within 6° from the GRB position was compared to the background estimate based on the event rate in the same angular bin during a 7 hr period including the GRB.

A negative fluctuation of $\approx 0.6\sigma$ was found. We then derived a 90% C.L. upper limit on the number of signal events following the method of Feldman and Cousins [20]. The limit was then converted to flux units using a Monte Carlo simulation of the detector response. Assuming a power law spectrum with a cutoff at 100 GeV, the upper limit on E^2 dN/dE at 65 GeV is $8.6 \cdot 10^{-4}$ erg/cm^2. For a spectrum extending up to 316 GeV, the limit on the $>$100 GeV emission is $1.5 \cdot 10^{-4}$ erg/cm^2 at 208 GeV.

A similar analysis was applied to VAMOS data for GRB 120328B. Shower events were selected within a 7° radius bin centered at a location corresponding to the center of the improved IPN error box (RA, Dec = 229.202°, +24.818°, based on data from [21]). A $+2\sigma$ fluctuation was found in a 30 s time window following GRB onset (06:26:23 UT). Consequently, and due to a less favorable zenith angle, the obtained limits are weaker than for GRB 111016B: $3.3 \cdot 10^{-3}$ erg/cm^2 at 141 GeV (100 - 200 GeV band) and $1.4 \cdot 10^{-3}$ erg/cm^2 at 283 GeV (200 - 400 GeV band). The limits have been corrected by a factor of 1.6 to account for systematic uncertainties in the signal detection efficiency. The data complement the spectral measurements made at lower energies by *Fermi* LAT.

For GRBs in HAWC's FoV, a circular bin with a radius of 4° was defined for each GRB using its equatorial coordinates. Two time windows were used: one for prompt emission that is equal to the satellite-measured T90, the time over which a burst emits from 5% of its total measured counts to 95%, and a second one that is 3$\times$ longer (to cover extended emission). Both time windows used the same start time (see Table 1). The number of events observed in the search bin defined by the 4° circle and the chosen time window was compared to the background estimated from off-time data.

When measured at a constant location in detector coordinates (zenith and azimuth), HAWC's background level is very stable on time scales relevant for GRBs. This allows us to predict the background in a circular bin around any source location at any given time. For a finite

1. http://gcn.gsfc.nasa.gov/gcn3 archive.html
2. http://heasarc.gsfc.nasa.gov/W3Browse/all/fermigbrst.html
3. http://heasarc.nasa.gov/docs/swift/archive/grb_table/

GRB Name	R.A.	Dec.	Inst.	Start Time (UT)	T90 (s)	Zenith Angle (°)	Bkg (evts/T90)	# Sig Evts for 5σ det.
121209A	21:47:8.93	-8:14:7.1	Swift	21:59:11	42.7	31.1	793.4	145.3
121211A	13:02:7.99	30:08:54.9	Swift	13:47:02	182.0	12.2	7329.8	428.2
130102A	20:45:41.63	49:49:03.5	Swift	18:10:54	77.50	40.7	835.6	149.1
130131511	12:38:31.2	-14:28:48	Fermi	12:15:17.0	147.50	43.2	1881.1	216.9
130215A	02:53:56.64	13:23:13.2	Swift	01:31:27	65.70	26.8	2788.2	264.8
130216A	04:31:36.24	14:40:12	Swift	22:15:21	6.50	42.5	95.6	53.1
130219A	20:14:55.2	40:49:48	Fermi	18:35:52.4	96.10	32.3	2886.4	269.6
130224370	13:43:36.0	59:43:12	Fermi	08:52:26.5	70.90	42.2	1017.6	160.4
130307126	10:23:59.0	22:59:53	Fermi	03:01:44.4	0.40	40.1	6.99	17.7
130327A	06:08:9.28	55:42:53.3	Swift	01:47:30	9.00	40.4	188.0	72.7
130504C	06:06:31.3	+03:50:02	Fermi	23:29:06.2	73.2	29.8	3205.8	283.2
130507545	21:18:57.6	-20:31:48	Fermi	13:04:38.0	60.2	39.8	1317.83	182.2

Table 1: Results for search for high-energy HAWC GRBs. The first 6 columns show the GRB name, the best available localization (RA, Dec), the relevant instrument (*Swift* or *Fermi*), the start time of the T90 analysis window, and the T90 itself (*Swift* BAT or *Fermi* GBM). The seventh column gives the GRB zenith angle at HAWC. The number of events per T90 is shown in the eighth column while the last column gives the number of signal events needed for 50% probability of a 5σ detection for the background in the previous column.

time window, the background expectation is the integral of the background rate over the time window duration, which implies integration along the visible trajectory of the source in the detector field of view. It is easy to see that shifting the source in time by T and the source RA by the corresponding angle in RA will place it at the same zenith and azimuth as the original source. This provides a natural way to estimate the background from off-time data. In this analysis we use a series of "test source" locations that covers an 8 hr interval around the GRB. The background estimates obtained using this method for the T90 time window are shown in Table 1.

The required number of signal events in the T90 time-window for 50% Poisson probability of a 5σ detection, given the number of background events, is displayed in the ninth column of Table 1. The number of counts in each time-window for each GRB does not exceed the required number of events for a 5σ detection. The measurements for all selected GRBs are thus consistent, within 5σ, with statistical fluctuations of the background. These results are preliminary. To ensure blindness for future analyses, the exact number of events seen in the signal time-window is not given.

For GRB 130504C, a 105 s time window was used in addition to the T90 and 3×T90 windows from the prescription. This matches the time of the fluence given by Konus-Wind (GCN circular 14578), which provides a spectral fit for comparison. Figure 2 shows the upper limits set by the 5σ discovery requirement of the analysis for GRB 130504C. The energy bands are the same as those used for GRB 111016B. Analyses that will improve this limit are in progress.

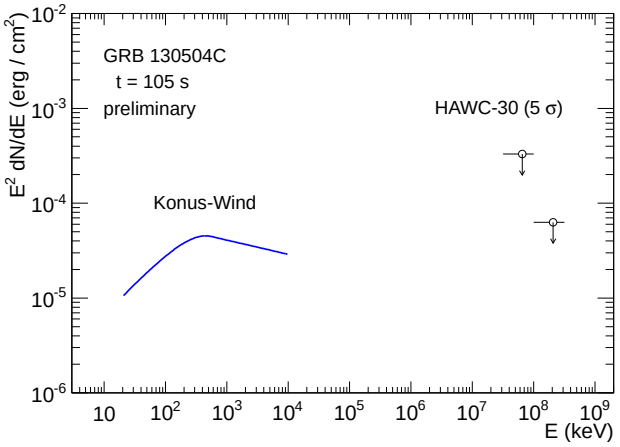

Fig. 2: The 5σ upper limit on high-energy emission from GRB 130504C imposed by HAWC data. 5σ sensitivity is reported rather than 90% C.L. upper limits to allow the data to remain blind. The spectral fit reported by Konus-Wind (GCN circular 14578) is shown for comparison.

5 Future analyses

In addition to the single time-bin technique described above, two other more complex analyses are being developed for main DAQ data: (1) a model-dependent likelihood analysis and (2) a model-independent scanning time-window analysis.

The maximum likelihood analysis takes advantage of information from other instruments and theoretical models of GRBs. The probability density function (PDF) for the GRB light curve is derived from knowledge of each specific GRB with parameter boundaries appropriately reflecting the high-energy spread seen in the the *Fermi* LAT GRB catalog. The background rate is determined with off-time data. An extended likelihood function is then constructed from the model of the signal and background PDFs and numerically maximized with respect to the number of signal events using MINUIT[4].

To determine the significance of discovery, we consider the standard likelihood ratio test statistic:

4. http://lcgapp.cern.ch/project/cls/work-packages/mathlibs/minuit/doc/doc.html

$$D = -2\log\left[\frac{\mathscr{L}(n_s = 0)}{\mathscr{L}(\hat{n}_s)}\right]$$

where $\hat{n}_s$ is the best fit value for the number of signal events. The maximum likelihood value produced with the model is compared to the null hypothesis, i.e. a model that does not include signal from the GRB. This tests how often background mimics signal. We use the cumulative distribution of D for simulated background-only light curves to determine the probability that a measured signal under the null hypothesis is simply a statistical fluctuation of the background. This analysis is currently underway and will be subject of a future publication.

Unlike the model-dependent likelihood method, the other HAWC technique for GRB detection does not rely on outside sources of information. It scans the full sky continuously with a set of time windows that cover the range of known GRB durations looking for upward fluctuations in the expected background rate. Trial factors are accounted for using the distribution of probabilities from the full search.

While this technique is intended to work online in the future, it is being run offline on known GRBs at this time. Once a GCN notice is released, we take the start time T0 and location of the burst and begin an automated, predefined search. Data within the uncertainty of the reported location are tiled for a spatial search with N single-duration time windows shifted from T0 until the GRB is beyond HAWC's FoV. The trials-corrected significance of the search result is calculated using simulation.

6 Outlook for HAWC GRB sensitivities

As the detector array continues to grow, the sensitivity of HAWC increases dramatically. Figure 3 illustrates the effects of different GRB emission spectra on the expected sensitivity of HAWC for several construction phases using the single time-bin analysis. We consider a burst at a zenith angle of 20°, lasting one second, with a spectrum of the type dN/dE $\propto E^{-\gamma}$ with a range of indices for 3 different high-energy cutoffs. The effect of the EBL is not directly considered because it can be simplistically simulated by the sharp cutoff. As an example, for a redshift of $z = 1$, Gilmore et al. [8] predict a cutoff at about 125 GeV. Data for GRBs 090510, 090902b, and 130427a, extracted from [10], [11], and [23], are shown for comparison.

HAWC stands an excellent chance of seeing a GRB based on those seen by *Fermi* LAT. For example, even if the source spectra or EBL causes the gamma rays to cutoff above 100 GeV, the full HAWC array will still be able to see such bursts as those shown in Figure 3.

Physics operations with 440 PMTs is expected to begin in August 2013. HAWC-250 (1,000 PMTs) is on schedule for completion in August 2014. Even before the array becomes complete at the end of 2014, HAWC is extremely sensitive to high-energy GRBs.

Acknowledgment: We acknowledge the support from: US National Science Foundation (NSF); US Department of Energy Office of High-Energy Physics; The Laboratory Directed Research and Development (LDRD) program of Los Alamos National Laboratory; Consejo Nacional de Ciencia y Tecnología (CONACyT), México; Red de Física de Altas Energías, México; DGAPA-UNAM, México; and the University of Wisconsin Alumni Research Foundation.

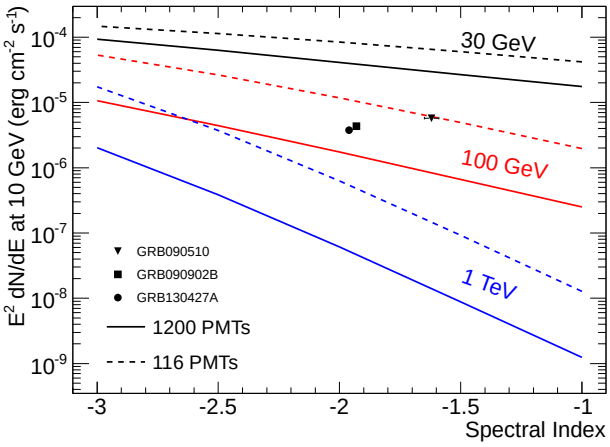

Fig. 3: The 5σ discovery potential for various values of a sharp high-energy spectral cutoff as a function of spectral index for HAWC with 116 PMTs and 1200 PMTs. The duration of the burst is fixed to 1 s and the zenith angle is fixed to 20°. Data from 3 different GRBs are corrected for the sensitivity to duration and inserted for comparison [10, 11, 23].

References

[1] M. Ruffert et al., A&A 344 (1999) 573-606
[2] S. Rosswoget al., MNRAS 345 (2003) 1077-1090
[3] S. E. Woosley, ApJ 405 (1993) 273-277
[4] A. MacFadyen et al., ApJ 524 (1999) 262
[5] P. Mészáros, Science 291 (2001) 79-84
[6] P. Mészáros, Rept. Prog. Phys. 69 (2006) 2259
[7] T. Piran, Physics Reports 314 (1999) 575-667
[8] R. C. Gilmore et al., MNRAS 399 (2009) 1694-1708
[9] D. Band et al., ApJ 413 (1993) 281
[10] M. Ackermann et al., ApJ 716 (2010) 1178-1190
[11] A.Abdo et al., ApJ 706 (2009) L138
[12] Fermi-LAT Collaboration, arXiv:1303.2908 [astro-ph.HE].
[13] J. Hinton, New J. Phys. 11 (2009) 055005
[14] G. Sinnis, New J. Phys. 11 (2009) 055007
[15] S. Vernetto, GRB Coordinates Network (GCN): A Status Report
[16] D. Lennarz et. al., paper 1160 (these proceedings)
[17] HAWC Collaboration, Astropart. Phys. 35, 641 (2012)
[18] J. Goodman et. al., paper 0702 (these proceedings)
[19] Yi-Zhong Fan et al., arXiv:1305.1261 [astro-ph.HE]
[20] G. J. Feldman, R. D. Cousins, Phys. Rev. D 57 (1998), 3873-3889
[21] K. Hurley, private communication
[22] Williams D. A. et. al., AIP Conf. Proc. 921, p476 (2007)
[23] S. Zhu, GRB Coordinates Network (GCN) Circular 14508